Evidence for strong magnetoelastic effects in Ni nanowires embedded in polycarbonate membranes

S. Dubois and J. Colin
Laboratoire de Métallurgie Physique, SP2MI, Boulevard 2, Teleport 2, 86960 Futuroscope Cedex, France

J. L. Duvail
IMM, Laboratoire de Physique Cristalline, BP 32229, 44322 Nantes Cedex 3, France

L. Piraux
Unité PCPM, Place Croix du Sud 1, 1348 Louvain la Neuve, Belgium
(Received 8 December 1999)

The uniaxial anisotropy energy of arrays of submicronic (30–500 nm) Ni wires synthesized by electrodeposition into cylindrical pores of track-etched polycarbonate membranes is studied as a function of temperature. At room temperature, the uniaxial anisotropy is equal to the shape anisotropy whereas an additional contribution, that reinforces the wire axis as an easy axis is evidenced at low temperature. This additional contribution is demonstrated to find its origin in magnetoelastic effects conjointly induced by the Ni and polycarbonate thermal-expansion coefficients mismatch and by the low volume fraction of Ni in Ni/polycarbonate samples.

I. INTRODUCTION

Mainly motivated by technological interests involving the miniaturization of sensors and the continuous increase of the magnetic storage density, techniques for fabrication (such as nanolithography) and characterization (near field microscopy, electronic microscopy, etc.) of magnetic nanoscaled systems have been developed.[1] To date, physical vapor deposition techniques followed by lithography of ever increasing resolution are usually considered to represent the ultimate technique for producing nanoscale magnets. However, well crystallized nanomagnets can also be fabricated using a different method whose key ingredients are ''template and electrodeposition'' techniques.[2] In this method, thin wires of magnetic metals with extremely large aspect ratios are electrochemically synthesized within the voids of alumine media[3] and track-etched polymer membranes.[4] Magnetic order and reversal processes which have been extensively studied since the turn of the century are consequently being reexamined for nanostructured magnets. Interesting properties are expected as the geometrical dimensions of the wires become comparable to the characteristic nanoscopic length scales such as domain wall width, exchange length, and mesoscopic dimensions such as domain width. Ideally, one would like to study an individual and isolated particle to avoid effects arising from particle size variations and dipolar interactions between particles. However, measuring the magnetization of a single nanometer-scale particle is beyond the limits of traditional magnetometers. Nevertheless, using microsuperconducting quantum interference devices (SQUID's) (Ref. 5) and magnetic force microscopy MFM,[6] magnetization reversal studies of individual Ni nanowires (free from the polymer membrane) have been performed. However, μSQUID's measurements are limited to low temperature and MFM measurements have been performed at room temperature. Anisotropic magnetoresistance (AMR) measurements performed on a single wire embedded in the polymer membrane were also used as a probe of the magnetization orientation with respect to the current.[7] Such a technique is well suited to investigate magnetization reversal and switching fields as a function of temperature.

Interestingly, it was shown that the presence of the polymer membrane around the magnetic nanowires changes the magnetic properties as the temperature is decreased.[8] It is suggested in Ref. 9 that the Ni and polycarbonate (PC) thermal expansion coefficients mismatch induces magnetostrictive effects. In these systems, the temperature dependence of switching fields may be strongly modified due to an additionnal contribution to the anisotropy.

In this paper, we present results of uniaxial anisotropy energy measurements at 300 and 35 K on arrays of Ni nanowires of different diameter. Next, x-ray-diffraction (XRD) analysis is performed to investigate the axial deformation of Ni wires upon cooling. Finally, an elastic model is formulated to calculate the stress and deformation components of Ni wires embedded in PC membranes. Magnetoelastic contributions are then calculated and compared to experimental data.

II. EXPERIMENTAL DETAILS

Arrays of Ni nanowires were synthesized by electrodeposition in track-etched polymer membranes following the same procedure as the one described by Withney *et al.*[4] However, in the present work, the host matrix consists in nanoporous PC membranes produced at the lab scale.[10] These membranes exhibit improved properties in terms of pore shape, pore orientation, pore size distribution, and pore surface roughness. As a result, Ni nanowires are almost perfectly cylindrical, parallel (deviation less than $\pm 5°$), and present a low roughness on their surface. The pore density and pore diameter of the different PC membranes used in this study are in the range $[7\times10^6, 2\times10^9]$ cm^{-2} and [500, 30] nm, respectively. Membrane thickness (i.e., wire length)

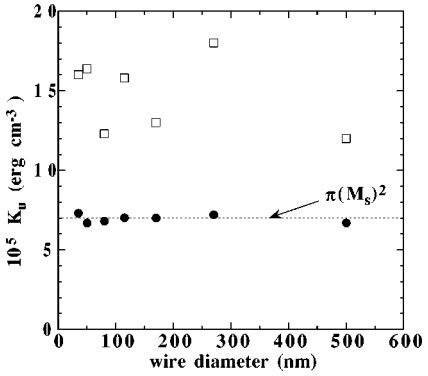

FIG. 1. Uniaxial anisotropy energy at 300 K (closed circles) and 35 K (open squares) as a function of wire diameter. The dashed line indicates the shape anisotropy.

is 20 μm. As the average spacing between wires is always larger than about five times the wire diameter, magnetic interactions between Ni wires are expected to be small.[11] For XRD analysis, arrays of Ni wires are glued on a silicon single crystal to avoid parasitic diffraction and diffusion from the support.

III. RESULTS AND DISCUSSION

Magnetization measurements have been performed on the different arrays of Ni wires. For the different samples under study, hysteresis loops have been measured with an external field applied parallel and perpendicular to the wire axis. Thus the uniaxial anisotropic energy, represented as a function of the wire diameter in Fig. 1, has been estimated from the change in magnetization work calculated for applied field parallel and perpendicular to the wire axis.[12] At room temperature, a value of about 7.0×10^5 erg cm^{-3} is calculated whatever the wire diameter. This value almost exactly corresponds to the shape anisotropy energy $\pi M_s^2=7.4\times10^5$ erg cm^{-3} (with $M_s=485$ Oe for Ni at 300 K) of an infinite Ni cylinder. As dipolar interactions between wires and magnetocrystalline anisotropy can be neglected in our systems, internal tensile stresses, which are known to appear during Ni films electrodeposition,[13] do not induce any significant magnetoelastic contribution to the anisotropy in the Ni wires. As a consequence, it can be considered that, at room temperature, the single contribution to the anisotropy comes from the shape. At low temperature, the uniaxial anisotropy energy increases. As the shape anisotropy is almost temperature independant (neglecting the slight variation of M_s), the additional contribution to the anisotropy energy (K_{excess}) can be easily calculated with the following relation $K_{excess}=K_u-7.0\times10^{+5}$ erg cm^{-3}.

As suggested in Ref. 9, this extra-uniaxial anisotropy may be related to the presence of the polycarbonate membrane and to the chemical bonding existing between the polycarbonate matrix and Ni wires. Considering the large mismatch of the Ni and PC thermal expansion coefficients, thermal stresses and resulting magnetostrictive effects should be taken into account. X-ray-diffraction (XRD) analysis was then performed to investigate the possible texture of the Ni nanowires, the Ni deformation induced upon cooling and the consequence on the magnetoelastic energy. Figure 2 shows

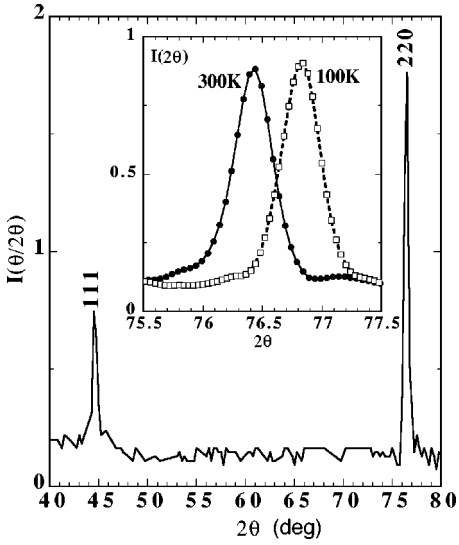

FIG. 2. $\theta/2\theta$ XRD spectrum recorded at 300 K on an array of wires (diameter 75 nm). Inset: (220) peaks recorded in symetric mode at room temperature (full line, black circles) and at about 100 K (dotted line, empty squares).

the $\theta/2\theta$ spectrum recorded at room temperature on an array of Ni wires (diameter: 75 nm). The intensities ratio of the 220 and 111 diffraction lines, $I_{220}/I_{111}=2.8$, gives evidence for a strong texture, $\langle110\rangle$ being the preferentially growth direction. Indeed, this ratio is expected to be 0.2 for a nontextured sample. We additionally record rocking curves on the 220 and 111 peaks to characterize the strength of the texture. The full width at half maximum is about 10° on the 220 peak which means, assuming a Gaussian distribution, that 75% of the wires have an orientation within 5° of that direction. The rocking curve recorded on the 111 peak reveals a fiber texture, suggesting an isotropic behavior in the plane perpendicular to the wire axis. Due to the existence of such a texture, we decided to investigate the displacement of the (220) peak in the symmetric mode and the displacement of the (311) and (222) peaks in the asymmetric mode. These peaks thus correspond to the grains with the $\langle110\rangle$ direction parallel to the wire axis. The inset of Fig. 2 shows the (220) peaks recorded at room temperature and at about 100 K. Displacement of the (220) peak gives evidence for a strong compressive stress in the wire axis direction. The relative variations of the interreticular distances d_{311} and d_{222} are also in agreement with such a compressive stress. Quantitatively, the relative variation of the interreticular distance (d_{220}) is about $-(0.45\pm0.05)\%$ which is larger than the expected variation due to the Ni thermal expansion coefficient (about -0.15%). Given the experimental deformation [$\epsilon=-(0.45\pm0.05)\%$] and the Young modulus in the $\langle110\rangle$ direction (230 GPa), one can calculate the compressive stress in the wire axis direction : $\sigma=E\cdot\epsilon=-1.03$ GPa. From the Ni magnetoelastic constants in the $\langle110\rangle$ direction, one can deduce the magnetoelastic anisotropy K_{me} through

$$K_{me}=\sigma^{Ni}[\lambda_{110}(M//\langle110\rangle)-\lambda_{110}(M\perp\langle110\rangle)] \qquad (1)$$

with $\lambda_{110}(M//\langle110\rangle)=-30\times10^{-6}$ and $\lambda_{110}(M\perp\langle110\rangle)=+7.3\times10^{-6}$ the magnetoelastic constants for magnetization lying parallel and perpendicular to the $\langle110\rangle$ direction, respectively.[14]

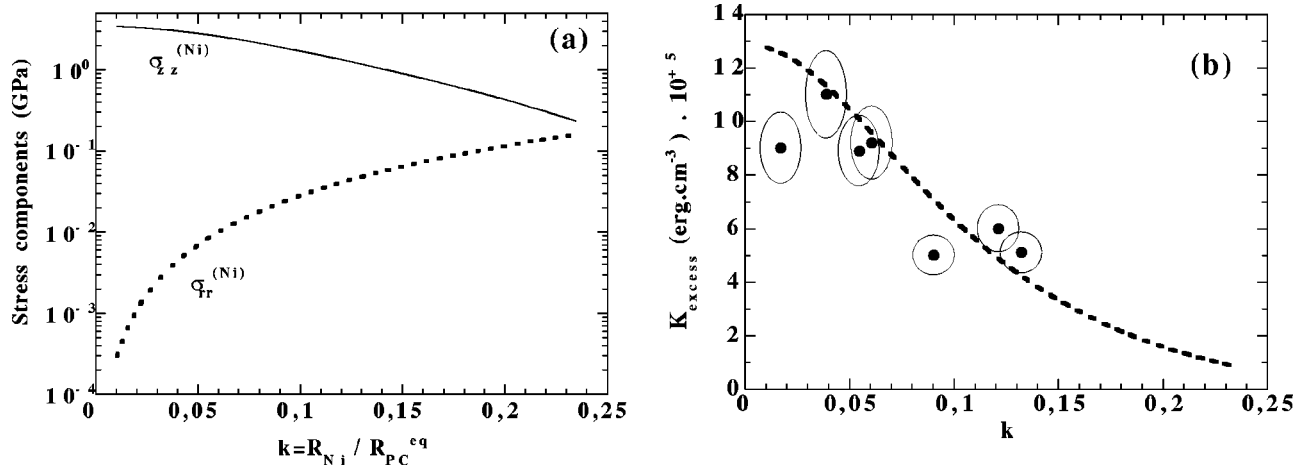

FIG. 3. Absolute values of the calculated stress components in Ni wires as a function of $k=R_{Ni}/R_{PC}^{eq}(a)$. Calculated magnetoelastic energy (dotted line) and experimental anisotropy excess (closed circles) vs k (b).

Equation (1) then leads to $K_{me}=(3.9\pm0.5)\times10^{+5}$ erg/cm^3 which is in very good agreement with the K_{excess} value ($4.3\times10^{+5}$ erg/cm^3) determined at 100 K from SQUID measurements. From XRD analysis, a large deformation is observed in the wire axis direction. Induced magnetostrictive effects give account of the experimental anisotropy excess. However, the origin of thermal stresses is still unclear as the Young's modulus of Ni and polycarbonate are so different (about 230 GPa for Ni and 3 GPa for polycarbonate) that the contraction of polycarbonate should not have a large influence on Ni. In order to check the possibility for the PC membrane to impose a so large stress on Ni wire, an isotropic elastic calculation has been performed to estimate stress and strain induced by the large mismatch between the Ni and PC thermal expansion coefficients. From the calculated stress components, the induced magnetoelastic energy is then calculated and compared to the experimental data.

The method of eigenstrain, already used to solve a number of problems in micromechanics of solids,[15] can be applied to our problem. This method consists in calculating elastic stresses and strains due to nonelastic strains which are induced, in our problem, by the difference between the Ni and PC thermal expansion coefficients.[16] Since the distance between the Ni nanowires is greater than the wire diameter, the elastic interaction between nanowires can be neglected.[15] Thus the study can be limited to an equivalent PC cylinder around a single Ni wire of radius R_{Ni}.

At $T_0=300$ K, the single Ni wire and the PC membrane are assumed to be in the reference equilibrium state. At low temperature, thermal contraction induces nonelastic strains which are given by $\epsilon_{zz}^{Ni,*}=\epsilon_{rr}^{Ni,*}=\alpha_{Ni}(T_0-T)=\alpha_{Ni}\Delta T$ in the free Ni cylinder and by $\epsilon_{zz}^{PC,*}=\epsilon_{rr}^{PC,*}=\alpha_{PC}\Delta T$ in the free PC matrix.

When the Ni cylinder is considered in the matrix, and at temperature T, the resulting elastic state due to the difference of nonelastic strain $\delta\epsilon^*=(\alpha_{PC}-\alpha_{Ni})\Delta T$ can be determined using an extension of the plane strain problem.[16] Considering that axial strains in the cylinder (ϵ_{zz}^{Ni}) and in the matrix (ϵ_{zz}^{PC}) are constant, the stress $\bar{\bar{\sigma}}^i(r)$ and displacement $\vec{u}^i(r)$ components can be expressed, in cylindrical coordinates, as

$$\sigma_{rr}^i(r)=\frac{A_i}{r^2}+B_i,$$

$$u_r^i(r)=\frac{1}{2\mu_i}\left[-\frac{A_i}{r}+(1-2\nu_i)B_i r\right]-\nu_i\epsilon_{zz}^i r,$$

$$\sigma_{\theta\theta}^i(r)=-\frac{A_i}{r^2}+B_i,\quad u_z^i(z)=\epsilon_{zz}^i z,$$

$$\sigma_{zz}^i(r)=2\nu_i B_i+2\mu_i(1+\nu_i)\epsilon_{zz}^i,$$

with $i=$Ni in the Ni cylinder and $i=$PC in the PC matrix.

A_i, B_i are elastic constants to be analytically calculated in Ni wire and in polycarbonate matrix, μ_i and ν_i are, respectively, the shear modulus and the Poisson's ratio of each material. In the Ni cylinder, the constant A_{Ni} must be zero to avoid the divergence of the σ_{rr} stress component. The other elastic constants A_{PC} and B_i have been determined considering the equilibrium conditions of forces and the continuity of displacement.[16]

The determination of the elastic relaxation has been performed to the first order in $\delta\epsilon^*$. Stress and deformation components were calculated as a function of the pertinent parameter ($k=R_{Ni}/R_{PC}^{eq}$) of the problem with R_{Ni} in the range ($0.01\,R_{PC}^{eq}-0.25R_{PC}^{eq}$). Absolute values of the axial and radial compressive stresses are plotted in Fig. 3(a). For k smaller than 0.15, the axial compressive stress (σ_{zz}^{Ni}) is at least one order of magnitude larger than the radial stress (σ_{rr}^{Ni}). Thus, a magnetoelastic energy is associated with the difference between the radial and axial stress. In a first approximation, magnetoelastic energy can be estimated from the axial compressive stress, neglecting the radial stress component.

The magnetoelastic energy (K_{me}) can be estimated from Eq. (1) and magnetostrictive constants. Considering the density of Ni nanowires ρ and the PC membrane radius (R_{PC}), the values of the radius ratio $k=R_{Ni}/R_{PC}^{eq}=\sqrt{\rho}R_{Ni}/R_{PC}$ have been calculated for the different samples. Experimental and calculated values of anisotropy energy, K_{excess} and K_{me} respectively, are then plotted as a function of $k=R_{Ni}/R_{PC}^{eq}$ in Fig. 3(b). Calculated values of K_{me} are in good agreement

with the experimental data. This result confirms that the temperature dependence of uniaxial anisotropy is effectively related to the axial elastic strain in the Ni wires and in the PC matrix. Our elastic model demonstrates that this strain is conjointly induced by the Ni and PC thermal expansion coefficients mismatch and by the low volume fraction of Ni in the Ni/PC samples.

IV. CONCLUSION

In summary, hysteresis loops of Ni nanowires arrays embedded in PC matrix have been analyzed to investigate the temperature dependence of the uniaxial anisotropy. At room temperature, the uniaxial anisotropy is dominated by the shape anisotropy whereas an additional anisotropy has been evidenced at low temperature. XRD analysis demonstrates that thermal stresses and induced magnetostrictive effects can give account of the anisotropy excess encountered at low temperature. Finally, the calculation of the thermal stress and deformation components demonstrates that magnetostrictive effect are conjointly induced by the PC and Ni thermal expansion coefficients mismatch and by the low volume fraction of Ni in our Ni/PC composites. As a consequence, magnetization reversal studies performed on elongated particles embedded in polymer membranes have to take into account an additional contribution to the anisotropy which reinforces the long axis as an easy direction for magnetization. The temperature-dependant magnetoelastic anisotropy should influence the switching fields.

The authors would like to thank E. Ferain and R. Legras for providing the nanoporous polycarbonate membranes used in this study and J. Grilhé, P. O. Renault, and A. Declémy for useful discussions. This work was partly supported by the Belgian Interuniversity Attraction Pole Program (PAI-IUAP P4/10) and by the European Commission under the Brite-EuRam program (Contract No. BRPR-CT95-0001).

[1] G. A. Gibson and S. Schultz, J. Appl. Phys. **73**, 4516 (1993); M. Ledermann, S. Schultz, and M. Ozaki, Phys. Rev. Lett. **73**, 1986 (1994); R. F. W. Pease and R. L. White, J. Vac. Sci. Technol. B **13**, 1089 (1995); M. Hehn, K. Ounadjela, J. P. Bucher, F. Rousseaux, D. Decanini, B. Bartenlian, and C. Chappert, Science **272**, 1782 (1996); S. Chou, P. Krauss, and L. Kong, J. Appl. Phys. **79**, 6101 (1996); E. Gu, E. Ahmad, S. J. Gray, C. Daboo, J. A. C. Bland, L. M. Brown, M. Rrhrig, A. J. McGibbon, and J. N. Chapman, Phys. Rev. Lett. **78**, 1158 (1997); S. Chou, Proc. IEEE **85**, 652 (1997).

[2] C. R. Martin, Adv. Mater. **3**, 457 (1991) and reference therein.

[3] S. Kawai and R. Ueda, J. Electrochem. Soc. **122**, 32 (1975); K. I. Arai, K. Ishiyama, Y. Ohoka, and H. W. Kang, J. Magn. Soc. Jpn. **13**, 789 (1989).

[4] T. M. Whitney, J. S. Jiang, P. Searson, and C. Chien, Science **261**, 1316 (1993).

[5] W. Wernsdorfer, B. Doudin, D. Mailly, K. Hasselbach, A. Benoit, J. Meier, J. Ph. Ansermet, and B. Barbara, Phys. Rev. Lett. **77**, 1873 (1996).

[6] M. Ledermann, R. O'Barr, and S. Schultz, IEEE Trans. Magn. **31**, 3793 (1995); R. O'Barr, M. Ledermann, S. Schultz, W. Xu, A. Scherer, and J. Tonucci, J. Appl. Phys. **79**, 5303 (1996).

[7] J. E. Wegrowe, D. Kelly, A. Franck, S. E. Gilbert, and J. Ph. Ansermet, Phys. Rev. Lett. **82**, 3681 (1999).

[8] J. Meier, A. Blondel, B. Doudin, and J. Ph. Ansermet, Helv. Phys. Acta **67**, 671 (1994).

[9] J. Meier, B. Doudin, and J. Ph. Ansermet, J. Appl. Phys. **79**, 6010 (1996).

[10] E. Ferain and R. Legras, Nucl. Instrum. Methods Phys. Res. B **131**, 97 (1997), and references therein.

[11] L. Piraux, S. Dubois, E. Ferain, R. Legras, K. Ounadjela, J. M. George, J. L. Maurice, and A. Fert, J. Magn. Magn. Mater. **165**, 352 (1997).

[12] B. D. Cullity, *Introduction to Magnetic Materials* (Addison Wesley, Reading, MA, 1972).

[13] K. G. Budinski, in *Surface Engineering for Wear Resistance* (Prentice-Hall, Englewood Cliffs, NJ, 1988).

[14] $\lambda_{110}(M//\langle 110\rangle)$ and $\lambda_{110}(M\perp\langle 110\rangle)$ can be calculated using magnetostrictive constants $\lambda_{s,100}$ and $\lambda_{s,111}$; see for example, R. M. Borzoth and R. W. Hamming, Phys. Rev. **89**, 865 (1953); P. K. Baltzer, *ibid.* **108**, 580 (1957).

[15] T. Mura, in *Micromechanics of Defects in Solids*, edited by S. Nemat-Nasser and G. A. Oravas (N. Nijhoff, Dordrecht, The Netherlands, 1987), and references therein.

[16] S. Timoshenko and J. N. Goodier, *Theory of Elasticity* (McGraw-Hill, New York, 1951).